# Flight testing verification of lateral-directional dynamic stability of gliding birds due to wing dihedral

*Chenhao Wei*
School of Aeronautic Science and Engineering, Beihang University, Beijing, China

*Gang Lin*
Department of Avionic Systems, Chinese Flight Test Establishment, Xi'an, China

*Jun Huang and Lei Song*
School of Aeronautic Science and Engineering, Beihang University, Beijing, China, and

*Howard Smith*
School of Engineering, Cranfield University, Bedford, UK

## Abstract

**Purpose** – Unlike conventional aircraft, birds can glide without a vertical tail. The purpose of this paper is to analyse the influence of dihedral angle spanwise distribution on lateral-directional dynamic stability by the simulation, calculation in the development of the bird-inspired aircraft and the flight testing.

**Design/methodology/approach** – The gliding magnificent frigatebird (*Fregata magnificens*) was selected as the study object. The geometric and mass model of the study object were developed. Stability derivatives and moments of inertia were obtained. The lateral-directional stability was assessed under different spanwise distributions of dihedral angle. A bird-inspired aircraft was developed, and a flight test was carried out to verify the analysed results.

**Findings** – The results show that spanwise distribution changing of dihedral angle has influence on the lateral-directional mode stability. All of the analysed configurations have convergent Dutch roll mode and rolling mode. The key role of dihedral angle changing is to achieve a convergent spiral mode. Flight test results show that the bird-inspired aircraft has a well-convergent Dutch roll mode.

**Practical implications** – The theory that birds can achieve its lateral-directional stability by changing its dihedral angle spanwise distribution may explain the stability mechanism of gliding birds.

**Originality/value** – This paper helps to improve the understanding of bird gliding stability mechanism and provides bio-inspired solutions in aircraft designing.

**Keywords** Dynamic stability, Locomotion mode, Dihedral angle, Bird-inspired aircraft, Gliding bird

**Paper type** Research paper

## Nomenclature

$A$ = characteristic matrix;
$B$ = control matrix;
$b$ = wing span (m);
$C_{D0}$ = drag coefficient at zero lift;
$C_{l\beta}$ = coefficient of rolling moment due to sideslip;
$C_{lp}$ = rolling damping moment coefficient;
$C_{lr}$ = coefficient of rolling moment due to the yawing angular velocity;
$C_{n\beta}$ = coefficient of yawing moment due to sideslip;
$C_{np}$ = coefficient of yawing moment due to the rolling angular velocity;
$C_{nr}$ = yawing damping moment coefficient;
$C_{y\beta}$ = coefficient of side force due to sideslip;

$C_{yp}$ = coefficient of side force due to the rolling angular velocity;
$C_{yr}$ = coefficient of side force due to the yawing angular velocity;
$g$ = gravitational acceleration (m/s2);
$I_x$ = inertia moment of the X component (kg m2);
$I_z$ = inertia moment of the Z component (kg m2);

$I_{zx}$ = inertia product of the XZ component (kg m2);
$m$ = mass (kg);
$p$ = rolling angular velocity (rad/s);
$q_*$ = dynamic air pressure (Pa);
$R$ = yawing angular velocity (rad/s);
$S$ = wing area (m2);
$U$ = control vector;
$V_*$ = trimmed flight speed (m/s);
$X$ = state vector;
$\alpha_*$ = angle of attack (deg);
$\beta$ = angle of sideslip (deg);
$\theta_*$ = angle of pitch (deg);
$\xi$ = damping ratio of the Dutch roll mode;
$\phi$ = roll angle (deg); and
$w_n$ = natural frequency of the Dutch roll mode.

## Introduction

Many bird species can perform stable gliding (Freguson-Lees and Christie, 2006). The frigatebird, hawk and falcon are some examples of such birds. One of these bird species' common points is that they have no vertical stabilizer. In the case of no vertical stabilizer, most aircraft without lateral-directional active control cannot achieve lateral-directional dynamic stability. It leads to the question that whether bird without vertical stabilizer is inherently lateral-directional stable.

Some researchers have suggested that gliding birds are inherently lateral-directionally unstable because of the absence of a vertical tail. Therefore, bird's flight must be maintained by the neuromuscular system (Smith, 1952; Brown, 1963; Dhawan, 1991). However, recent research, including flight tests on an unmanned aircraft inspired by a raven (Hoey, 1992) and a quantitative analysis of a live steppe eagle (Gillies *et al.*, 2011), have suggested that gliding birds may be inherently stable.

With regard to the lateral-directional stability mechanism analysis of gliding birds, Sachs attributed the origin of birds' stable gliding without a vertical stabilizer to the "size effect" (Gillies *et al.*, 2011). Sachs (2005) introduced dynamic stiffness as a precise measurement for yaw static stability. The analysed results show that bird wings can provide adequate restoring aerodynamic yawing moment (Sachs, 2005). Sachs discussed the influence of dihedral angle changing to lateral-directional aerodynamic coefficients (Sachs and Moelyadi, 2010). In his research, the dihedral angle of the pigeon model remained constant along the spanwise sense. However, wing dihedral angle of some bird species varies from proximal wing to distal wing. Abdulrahim developed a morphing aircraft inspired by gull and analysed the response characteristic of the aircraft (Abdulrahim and Lind, 2004). The aircraft's wing was divided into two parts and the aircraft has a vertical stabilizer. In summary, relevant research still needs further refined. In Song Lei's flying wing aircraft research (Song *et al.*, 2014; Song *et al.*, 2015; Song *et al.*, 2016), it is indicated that aircraft without a vertical stabilizer can achieve lateral-directional dynamic stability under suitable dihedral angle spanwise distribution. The analysed result was verified by flight testing (Song *et al.*, 2014; Song *et al.*, 2015).

Considering that both gliding birds and flying wing aircraft lack a vertical tail, the mechanism of the stability of gliding birds may be similar to that of flying wing aircraft. Combined with the analysis of the relevant researches which indicated that gliding birds have dynamic stability, this paper's authors believe that gliding birds can achieve lateral-directional dynamic stability by adjusting the spanwise distribution of dihedral angle. To prove the conjecture, the frigatebird (*Fregata magnificens*) was selected as the study object in this paper. The geometric model and the mass model of a gliding frigatebird were built. The characteristics of the lateral-directional locomotion modes under different dihedral angle spanwise distributions were obtained. An aircraft inspired by gliding frigatebird was developed and gliding flight experiment was conducted to verify the theoretical analysed results.

## Materials and methods

### Gliding stability analysis method

A gliding bird can be treated as a rigid body with six degrees of freedom that can rotate or translate along the axes illustrated in Figure 1. In the theory of flight mechanics, the flying process is described by kinematic and dynamic equations. To analysis the stability issue, the small disturbance hypothesis is usually used to linearize the aerodynamic force and moment terms in kinematic and dynamic equations. The aerodynamic force and moment terms are linearized as a sum of the reference value and a small disturbance value. By neglecting the derivatives of the symmetric forces and moments to the asymmetric motion variables and keeping the first-order terms, the kinematic and dynamic equations are transformed to the longitudinal and lateral-directional linearized small disturbance equations (Etkin and Reid, 1996). Therefore, the longitudinal and lateral-directional motions are decoupled and can be analysed separately.

The general form of the linearized small disturbance equations can be written as:

$$\dot{x} = Ax + Bu \quad (1)$$

where $x$ is the state vector, $A$ is the characteristic matrix, $B$ is the control matrix and $u$ is the control vector. If the control vector is zero, the equation can be used to analyse the response under a small disturbance in an uncontrolled gliding process. In this case, the lateral-directional linearized small disturbance equations are given by:

**Figure 1** Body axes of a gliding bird
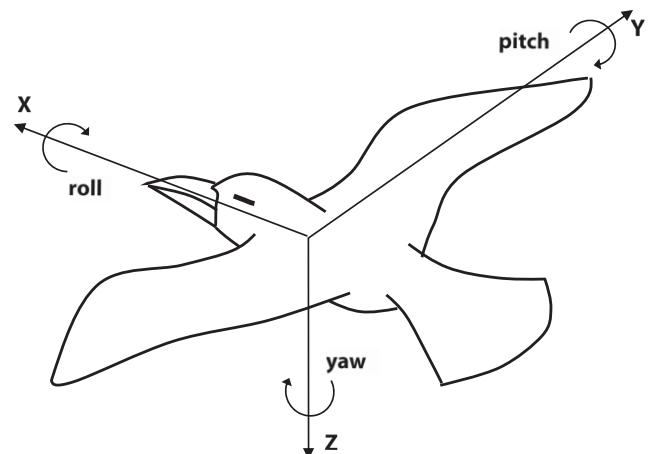
$$\begin{bmatrix} \dot{\beta} \\ \dot{p} \\ \dot{r} \\ \dot{\phi} \end{bmatrix} = \begin{bmatrix} \overline{Y}_\beta & \alpha_* + \overline{Y}_p & \overline{Y}_r - 1 & g\cos\theta_*/V_* \\ \overline{L}_\beta & \overline{L}_p & \overline{L}_r & 0 \\ \overline{N}_\beta & \overline{N}_p & \overline{N}_r & 0 \\ 0 & 1 & \tan\theta_* & 0 \end{bmatrix} \begin{bmatrix} \beta \\ p \\ r \\ \phi \end{bmatrix} \quad (2)$$

Here, $x = [\beta \; p \; r \; \phi]^T$, and the characteristic matrix $A$ is the matrix on the right-hand side of equation (2). Equation (2) consists of four sub-equations: side force equation, rolling angular velocity equation, yawing angular velocity equation and roll angle equation. The variables in matrix $A$ including $\overline{Y}_\beta$, $\overline{Y}_p$, $\overline{Y}_r$, $\overline{L}_\beta$, $\overline{L}_p$, $\overline{L}_r$, $\overline{N}_\beta$, $\overline{N}_p$ and $\overline{N}_r$ are the derivatives of the forces and moments with respect to motion variables. These derivatives can be calculated by the following equations:

$$\overline{Y}_\beta = \frac{C_{y\beta}q_* S}{mV_*}, \quad \overline{Y}_p = \frac{C_{yp}q_* S}{mV_*}\frac{b}{2V_*}, \quad \overline{Y}_r = \frac{C_{yr}q_* S}{mV_*}\frac{b}{2V_*}$$

$$\overline{N}_\beta = C_{y\beta}q_* Sb, \quad \overline{N}_p = C_{np}q_* Sb\frac{b}{2V_*}, \quad \overline{N}_r = C_{nr}q_* Sb\frac{b}{2V_*}$$

$$\overline{L}_\beta = C_{l\beta}q_* Sb, \quad \overline{L}_p = C_{lp}q_* Sb\frac{b}{2V_*}, \quad \overline{L}_r = C_{lr}q_* Sb\frac{b}{2V_*}$$

$$\overline{L}_i = \frac{L_i + (I_{zx}/I_z)N_i}{I_x - I_{zx}^2/I_z}, \quad \overline{N}_i = \frac{N_i + (I_{zx}/I_z)L_i}{I_z - I_{zx}^2/I_x}$$

where $C_{y\beta}$, $C_{yp}$ and $C_{yr}$ denote the side force coefficient due to sideslip, rolling and yawing, respectively. $C_{l\beta}$, $C_{lp}$ and $C_{lr}$ denote the rolling moment coefficient due to sideslip, rolling and yawing, respectively. $C_{n\beta}$, $C_{np}$ and $C_{nr}$ denote the yawing moment coefficient due to sideslip, rolling and yawing, respectively. $I_x$, $I_z$ and $I_{zx}$ denote the moments of inertia (kg m$^2$); $b$ denotes the wing span (m); $S$ denotes the wing area (m$^2$); $q_*$ denotes the dynamic air pressure (Pa); $V_*$ denotes the trimmed flight speed (m/s); and $m$ denotes the mass (kg). $\beta$, $r$ and $\phi$ are sideslip angle, rolling angular velocity, yawing angular velocity and roll angle, respectively. $\dot{\beta}, \dot{p}, \dot{r}$ and $\dot{\phi}$ are derivatives of these parameters to time.

As shown in equation (2), stability derivatives and moments of inertia are necessary to calculate the eigenvalues of the characteristic matrix. The stability derivatives under certain conditions can be obtained using a vortex lattice method (Song *et al.*, 2014). The moments of inertia can be estimated by building a mass model of the gliding bird. After entering the stability derivatives and moments of inertia into equation (2), the four eigenvalues of the characteristic matrix can be obtained. Each real eigenvalue or a pair of conjugate eigenvalues corresponds to a locomotion mode under a small disturbance. According to the flight mechanics theory, three typical modes including Dutch roll mode, the rolling mode and spiral mode exist in lateral-directional motion for aircraft. Considering that the flight condition of gliding bird is similar to that of aircraft, these three modes constitute the lateral-directional response of conventional aircraft and presumably gliding bird under a disturbance.

It is necessary to establish a set of criteria to evaluate the mode stability. For remotely piloted vehicle, the natural frequency, the damping ratio, the product of these two parameters above, time constant and the time to double the amplitude are used to assess the lateral-directional mode stability, and these parameters can be calculated based on the eigenvalues of the characteristic matrix. Specific stability criteria for these parameters are taken from the requirements described in detail in technical report AFFDL-TR-76–125 (Prosser and Wiler, 1976). These criterions are divided into three levels in the technical report and might be used as the reference value to evaluate gliding bird stability. Considering that the spiral mode belongs to the category of first-order motion and it may be convergent or divergent, a much clearer description of the spiral mode characteristics can be provided by using the eigenvalue magnitude rather than the time to double the amplitude. The sign of the eigenvalue determines whether the spiral mode is convergent or divergent. The magnitude of the eigenvalue determines the speed of the tendency to converge or diverge. Thus, the requirements for the time to double the amplitude can be transferred to the requirements defined by the eigenvalues.

In technical report AFFDL-TR-76–125 (Prosser and Wiler, 1976), the remotely piloted vehicles are divided into four class according to its weight and manoeuvrability level. The flight phases are divided into four categories. The stability levels are set associated with the pilot rating scale developed by Cooper and Harper (1969). The operator ratings are influenced by how hard the pilot has to complete the flight mission. The level 1 criterion means that operator remote control is clearly adequate to accomplish mission flight phase (Prosser and Wiler, 1976). After evaluating frigatebird flight condition, the level 1 criterion for small, light, remotely piloted vehicle in rapid manoeuvring flight phases was chosen as the reference criterion to evaluate the stability of frigatebird. The corresponding parameter requirements are 0.19 for the minimum value for the damping ratio, 1.0 rad/s for the minimum value for the natural frequency, 0.35 rad/s for the minimum value for the product of the natural frequency and damping ratio of Dutch roll mode, 1.0 for the maximum value for time constant of the rolling mode and 0.05775 for the maximum eigenvalue of the spiral mode.

## Frigatebird geometric modelling

The magnificent frigatebird (*Fregata magnificens*) was selected as the study object in this paper. The geometric model was used to calculate the stability derivatives. The model was constructed based on the physiological structure, photographs, videos and qualitative observation records of the gliding frigatebird (Marchant and Higgins, 1990).

The frigatebird geometric model includes the beak, trunk, tail and wings. The most significant appearance characteristics of each part were recorded and reflected in the modelling process. The geometric model's wing can be divided into three sections in the spanwise sense. The inner section sweeps back with a dihedral angle; the middle section sweeps forward with a slightly downwards inclination, and the outer section is flat and swept back. The dihedral angle in this paper is the angle between the projection of the leading edge on the vertical plane and the horizontal axis of the vertical plane. A combination of dihedral angles similar with observations was selected in the geometric modelling. The initial dihedral angle of the geometric model's wing is 38° for the inner section, −3° for the middle section and 0° for the outer section. The segmentation is shown in Figure 2(a).

The camber of the aerofoil used in the geometric model was optimized from the standpoint of the aerodynamic performance

**Figure 2** Frigatebird modelling



(a)

(b)

(c)

(d)
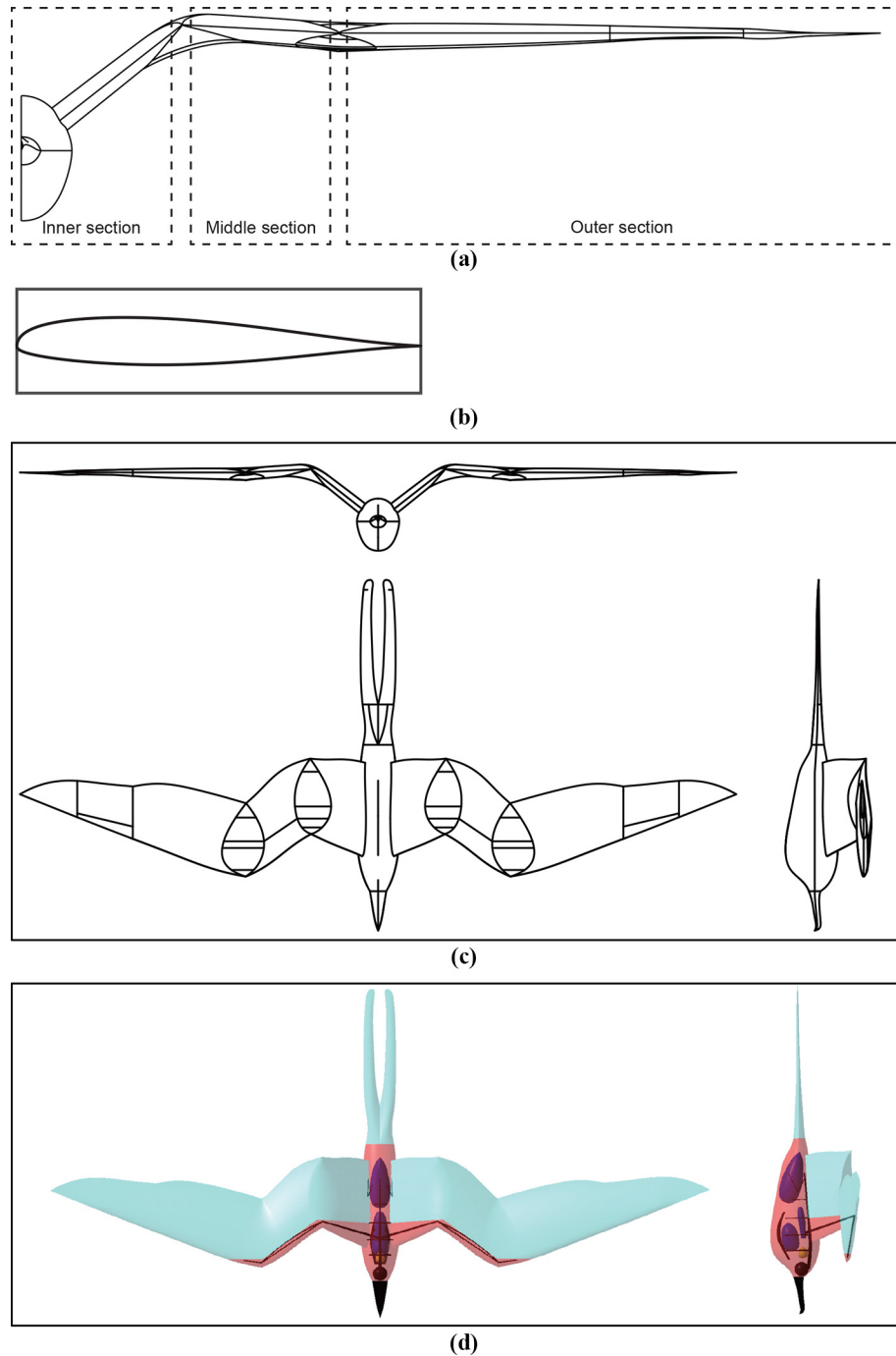
and manufacturing process. The maximum thickness ratio of the aerofoil is consistent with the Albatross aerofoil (Herzog, 1968). According to thin aerofoil theory, the aerofoil camber only affects the zero-lift angle of attack, and the lift-curve slope for all the aerofoil is the same in the linear lift-curve range (Anderson, 2017). The drag coefficients of the Albatross aerofoil and the aerofoil used in the geometric model were calculated by XFOIL. Under the condition that the trim lift coefficient is 0.57 and Reynolds number is 300000, the drag coefficient is 0.015 for the Albatross aerofoil and 0.011 for the aerofoil used in this paper. Little difference was

found between these two values. Based on DATCOM (Hoak, 1978), $C_{yp}$, $C_{lp}$, $C_{np}$, $C_{lr}$, $C_{l\beta}$ are affected by lift-curve slope of the aerofoil, and $C_{yp}$, $C_{lp}$, $C_{np}$, $C_{nr}$ are affected by $C_{D_0}$ among lateral-directional derivatives. Therefore, in the calculation of lateral-directional derivatives, the difference should be small between the effect achieved by using the aerofoil [Figure 2(b)] and the albatross aerofoil. In summary, the aerofoil may be a suitable alternative to real frigatebird aerofoil in the modelling process. The aerofoil [Figure 2(b)] used in the geometric model remains constant in the spanwise direction.

Figure 2(c) shows the geometric model. The configuration parameters of the frigatebird, as measured by previous studies, are summarized in Table 1 (Dhawan, 1991; Smith, 1984; Chatterjee and Templin, 2007; Koehl *et al.*, 2011; Brewer and Hertel, 2007; Pennycuick, 1983, 2008; Rogalla *et al.*, 2021). The geometric model's configuration parameters are also listed in Table 1. The geometric model's configuration parameters are consistent with the data measured by previous studies.

**Frigatebird mass modelling**

The mass model was built to estimate the moments of inertia. The mass model was divided into four parts, namely, feather, muscles, viscus and skeleton. The physiological morphology of each part analysed in previous studies (Dhawan, 1991; Schmitz *et al.*, 2018) was used as the reference data for the geometry establishment. The proportion of each part's weight to the total weight was also refers to the data in previous studies (Kuroda, 2004; Hamershock *et al.*, 1992; Whittow, 1999; Zheng, 2012).

In this paper, it is hypothesized that the feathers [Figure 2(d), grey part] represent 8% of the total weight; the skeleton [Figure 2(d), black part] represents 8% of the total weight; the heart [Figure 2(d), yellow part] represents 1% of the total weight; lungs [Figure 2(d), blue part] represent 2% of the total weight; and the muscles [Figure 2(d), red part] represent 81% of the total weight. Combining the geometry of each part, the moments of inertia were estimated. The moment of inertia about $x$-axes is $0.0401\,\mathrm{kg\,m^2}$; the moment of inertia about $z$-axes is $0.05147\,\mathrm{kg\,m^2}$, and the product of inertia about $x$- and $z$-axes is $-0.001077\,\mathrm{kg\,m^2}$. The model described above was defined as the base model and is shown in Figure 2(d).

**Vortex lattice method**

A vortex lattice method (Song *et al.*, 2014) was used to calculate the stability derivatives of the frigatebird model. The algorithm of the vortex lattice method during sideslip refers to the Tornado vortex lattice method calculation program, which was developed by Melin (2000). Song Lei modified the program in his study (Song *et al.*, 2014) for high computation rate and computation accuracy. In this paper, the method simplified the frigatebird model and retained its lift surface concluding wings and tail. The mean camber surface of the model's wing and tail was divided into serval vortex lattices. The aerodynamic forces applied to every section of the bound vortex line were calculated, and the force application points were set at the centre of each vortex section. After calculating the aerodynamic forces on each vortex lattice, the force and

moment of the object model could be obtained. The stability derivatives of the object model could be calculated by differentiating the aerodynamic forces and moments of different flying conditions.

With regard to drag, the method can calculate the induced drag while the form drag could not be obtained. Based on the aerodynamic calculations previously performed for aircraft, when the angle of attack and the angle of sideslip change slightly, the form drag of an aircraft is almost constant and thus will not significantly affect the stability of the aircraft.

The method was used to calculate the aerodynamic coefficients of a flying wing model, which is shown in Figure 3. The calculation results were compared with the wind tunnel experiment results to verify the method accuracy. The comparison results are shown in Figure 3. In this paper, the method is used to calculate the stability derivatives of the gliding frigatebird model. Considering that the morphology of gliding frigatebird is similar with that of flying wing aircraft, this method may be effective in this study.

Some fluid phenomena including leading edge vortex was not modelled in this paper. Bird flight is a complex process. The existence and form of the leading edge vortex are affected by numerous factors (Videler *et al.*, 2004; Muir *et al.*, 2017). It is generally considered that the effect of leading edge vortex is significant at high angles of attack (Lentink *et al.*, 2007). In our work, the analysis was conducted on the trimming condition of gliding birds. The angle of attack was under 8°. It might be inferred that leading edge vortex may have slight influence on the lateral-directional mode characteristic when angle of attack is kept at a small value. However, simulating the air flow of the flying bird with a higher fidelity will make the analysis results more reliable. Incorporating the leading edge vortices and other fluid phenomena into our model will be a very important research in the future.

**Bird-inspired aircraft development**

To verify the lateral-directional stability of the frigatebird model, an aircraft inspired by gliding frigatebird was developed. The configuration of the aircraft is consistent with the frigatebird geometric model. The three-view picture of the bird-inspired aircraft is shown in Figure 4(a). The aircraft's tail acts as an elevator [Figure 4(b)]. Ailerons are placed on the trailing edge of the wing [Figure 4(c)]. The aircraft has no power equipment, and it can glide in the sky. The aircraft photo is shown in Figure 4(d). The moments of inertia data for the aircraft were measured. The moment of inertia about $x$-axes is $0.1378\,\mathrm{kg\,m^2}$; the moment of inertia about $z$-axes is $0.1561\,\mathrm{kg\,m^2}$, and the product of inertia about $x$- and $z$-axes is $-0.0049\,\mathrm{kg\,m^2}$.

**Table 1** Frigatebird configuration data measured in previous studies and this paper

| Data sources | Span(m) | Aspect ratio | Mass(kg) | Wing loading (N/m$^2$) | Wing area(m$^2$) | Gliding speed (m/s) |
|---|---|---|---|---|---|---|
| **Koehl *et al.* (2011)** | – | – | 1.5 | 45 | – | 10 |
| **Brewer and Hertel (2007)** | – | 11.3 | 1.5 | 43 | – | – |
| **Smith (1984)** | 2.02 | 12.6 | 1.62 | 49 | 0.324 | 7.4 |
| **Pennycuick (1983)** | 2.29 | 12.8 | 1.52 | 36.5 | 0.408 | – |
| **Chatterjee and Templin (2007)** | 2.86 | 25.24 | 1.5 | 45.42 | 0.324 | 10 |
| **Pennycuick (2008)** | 2.14 | 12.3 | 1.67 | – | 0.372 | – |
| **Rogalla (2021)** | 2.29 | – | 1.47 | 35.3 | 0.408 | 8.2 |
| *This paper* | 2.19 | 11.4 | 1.5 | 35 | 0.42 | – |

**Figure 3** Results comparison between the vortex lattice method and wind tunnel experiment
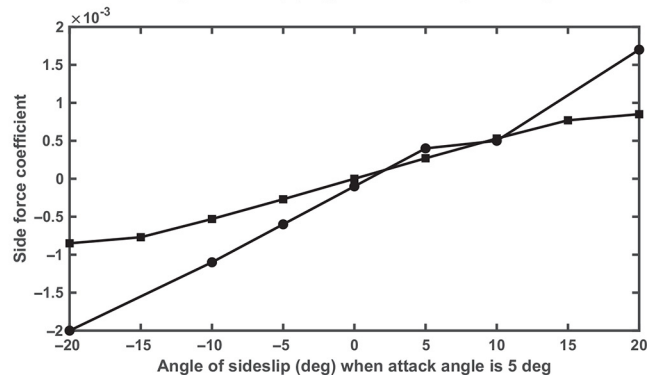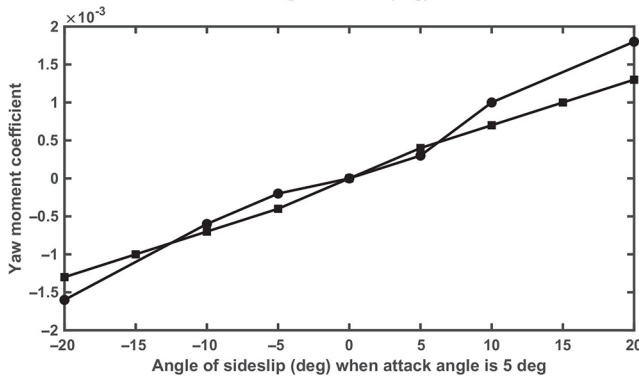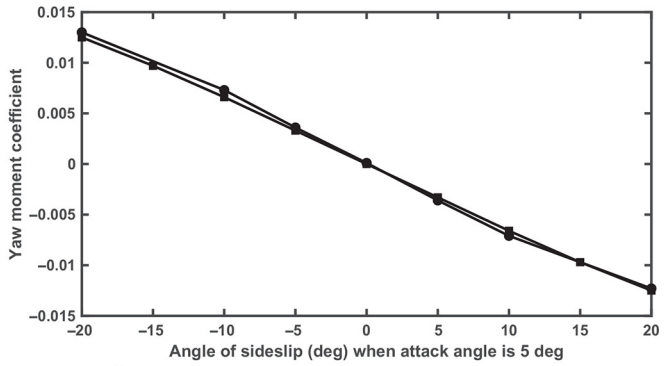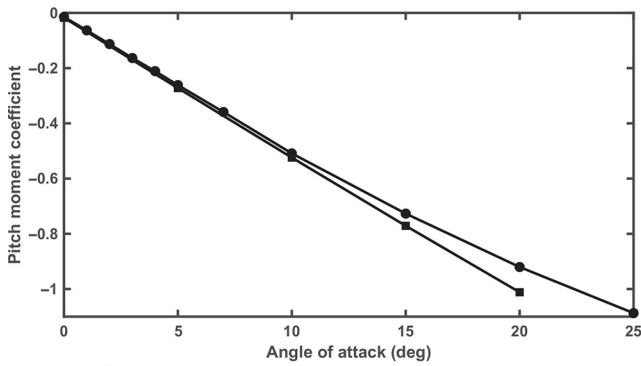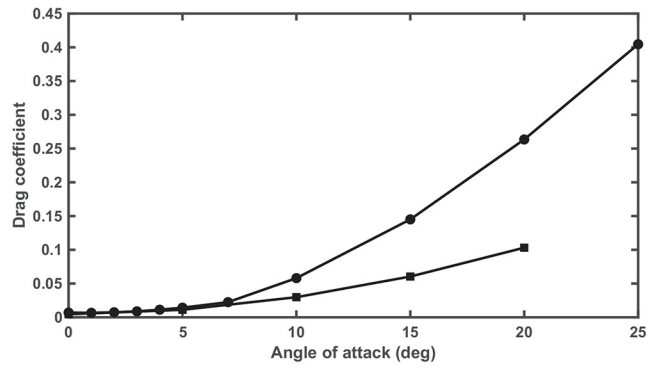
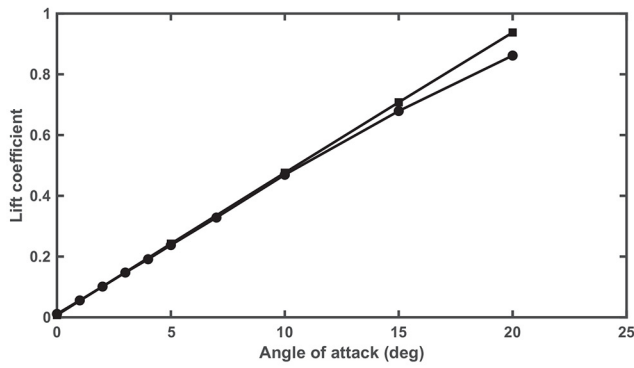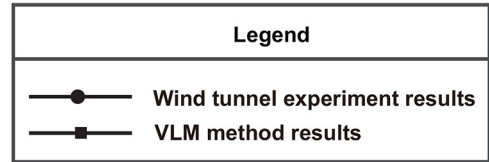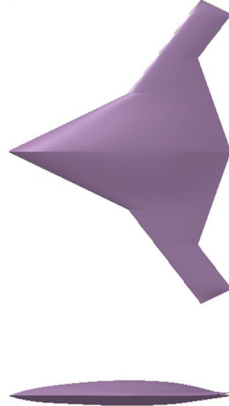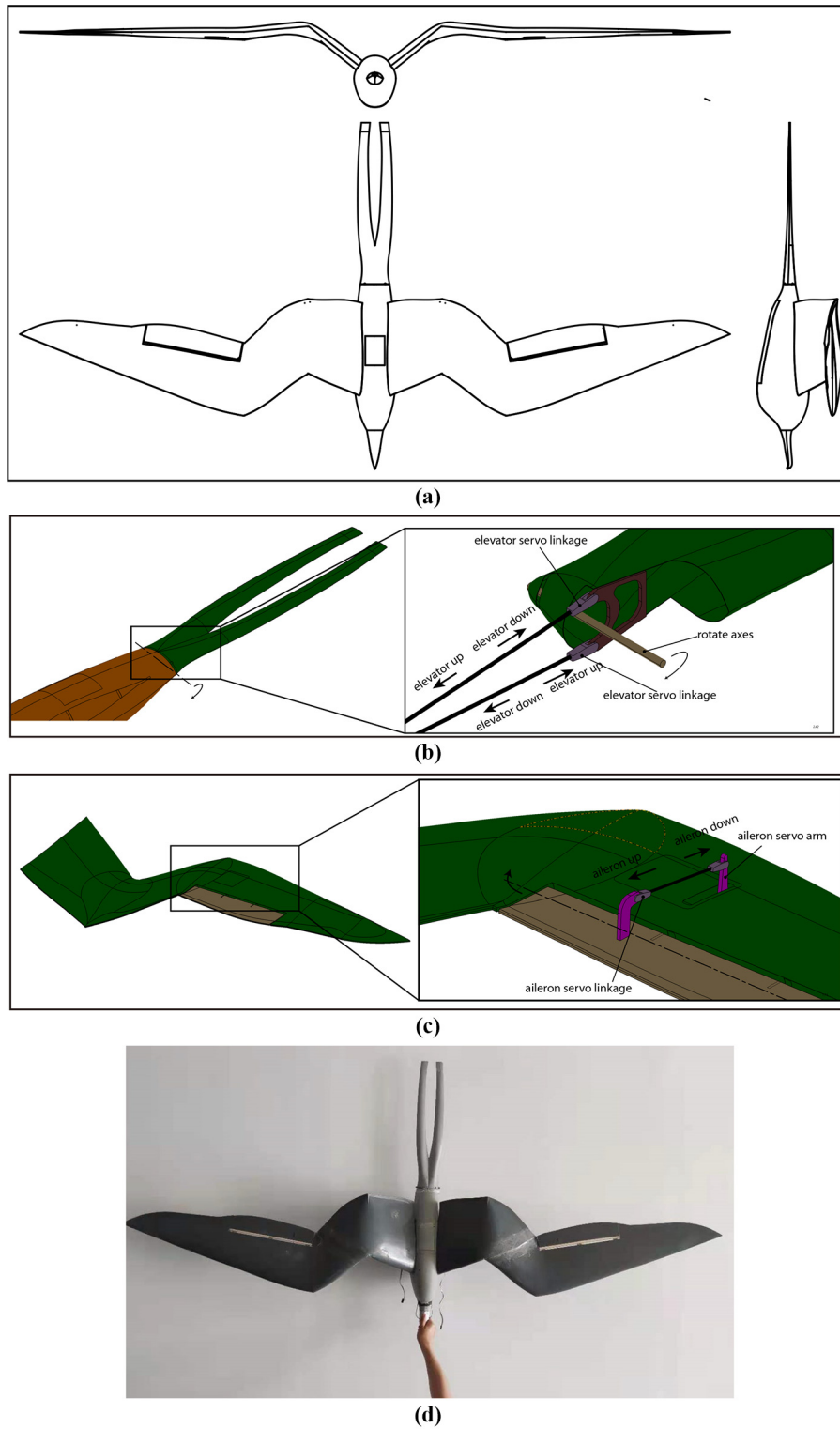**Figure 4** Aircraft inspired by gliding frigatebird



(a)

(b)

(c)

(d)

### Flight experiment

The flight experiment was conducted to verify the lateral-directional stability of the bird-inspired aircraft. The aircraft was catapulted to a certain speed by a bungee rope [Figure 5(a)]. After the rope separate itself from the aircraft, the aircraft climbed to a certain height and then began to glide. The flight experiment was carried out outdoors with no winds. The avionics placed in the aircraft record the flight data including the global positioning

**Figure 5** Flight experiment
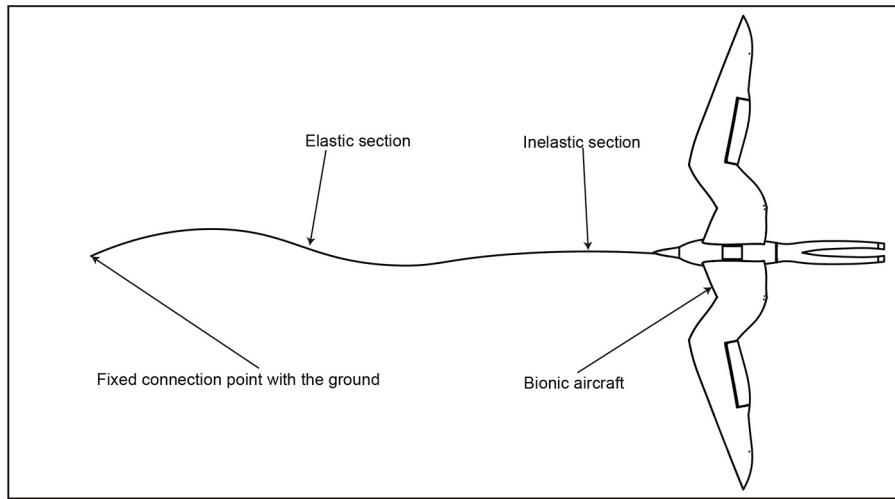


**(a)**
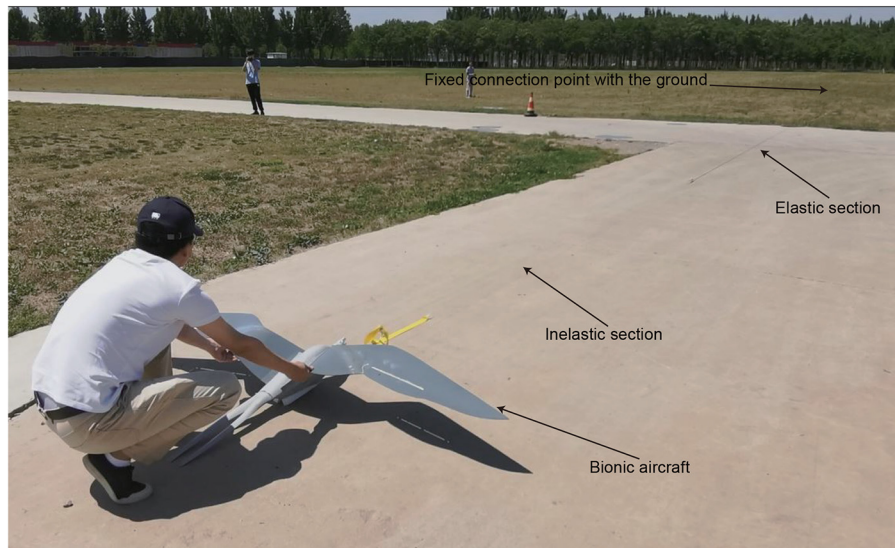


**(b)**

system (GPS) velocity, GPS height, control surface deflection signal, sideslip angle, roll angle, yaw angle, roll angular rate and yaw angular rate. Specifically, sensor module was used to measure flight data, and "Pixracer" flight control module was used to integrate, record and process flight data. The corresponding sensors and its accuracy are listed in Table 2.

The flight experiment includes two parts. The first part is the gliding with no lateral-directional control input. This part aims to prove the aircraft can perform a stable gliding. The second part is the gliding with a doublet excitation induced by ailerons. Flight data is recorded, and the parameters of the Dutch roll mode is identified. The identified results are compared with the

**Table 2** Accuracy of the sensors used in the flight experiment

| Sensor | Sensor type | Parameters measuring | Accuracy |
|---|---|---|---|
| **Gyroscope** | MPU9250 | Angle | ±0.18° |
| | | Angular velocity | ±0.05 rad/s |
| **Accelerometer** | ICM20608 | Acceleration | ±0.08 m/s² |
| **GPS** | NEO-M8N | GPS velocity | ±0.05 m/s |
| | | GPS position | 2.5 m |
| **Barometer** | MS5611 | Atmospheric pressure | ±5 mbar |

**Note:** GPS = Global positioning system

theoretical analysed results to verify accuracy. The photo of the flight experiment is shown in Figure 5(b).

## Results

### Influence of variation in dihedral angle on lateral–directional dynamic stability

By changing the dihedral angle of each section of the base model's wing, the lateral-directional dynamic stability for each dihedral angle distribution can be assessed. The dihedral angle of

the base model's each wing section was changed within a certain range. The range of variation of the inner section's dihedral angle is 28°–44°, that of the middle section is −9°–12° and that of the outer section is −6°–19°. With an interval of 1°, a total of 9,724 configurations were assessed. According to the flight data measured by Weimerskirch *et al.* (2016), the velocity during the whole gliding process mostly varies between 8 m/s and 12 m/s. Thus, the lateral-directional mode stability is analysed at the velocities of 8 m/s, 10 m/s and 12 m/s. The vortex lattice layout of the frigatebird model is shown in Figure 6. Then, the

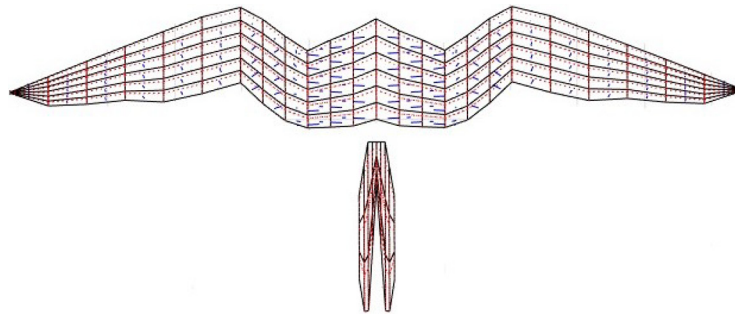**Figure 6** Vortex lattice layout of the frigatebird model



**Figure 7** Influence of dihedral angle changing on the natural frequency for Dutch roll mode
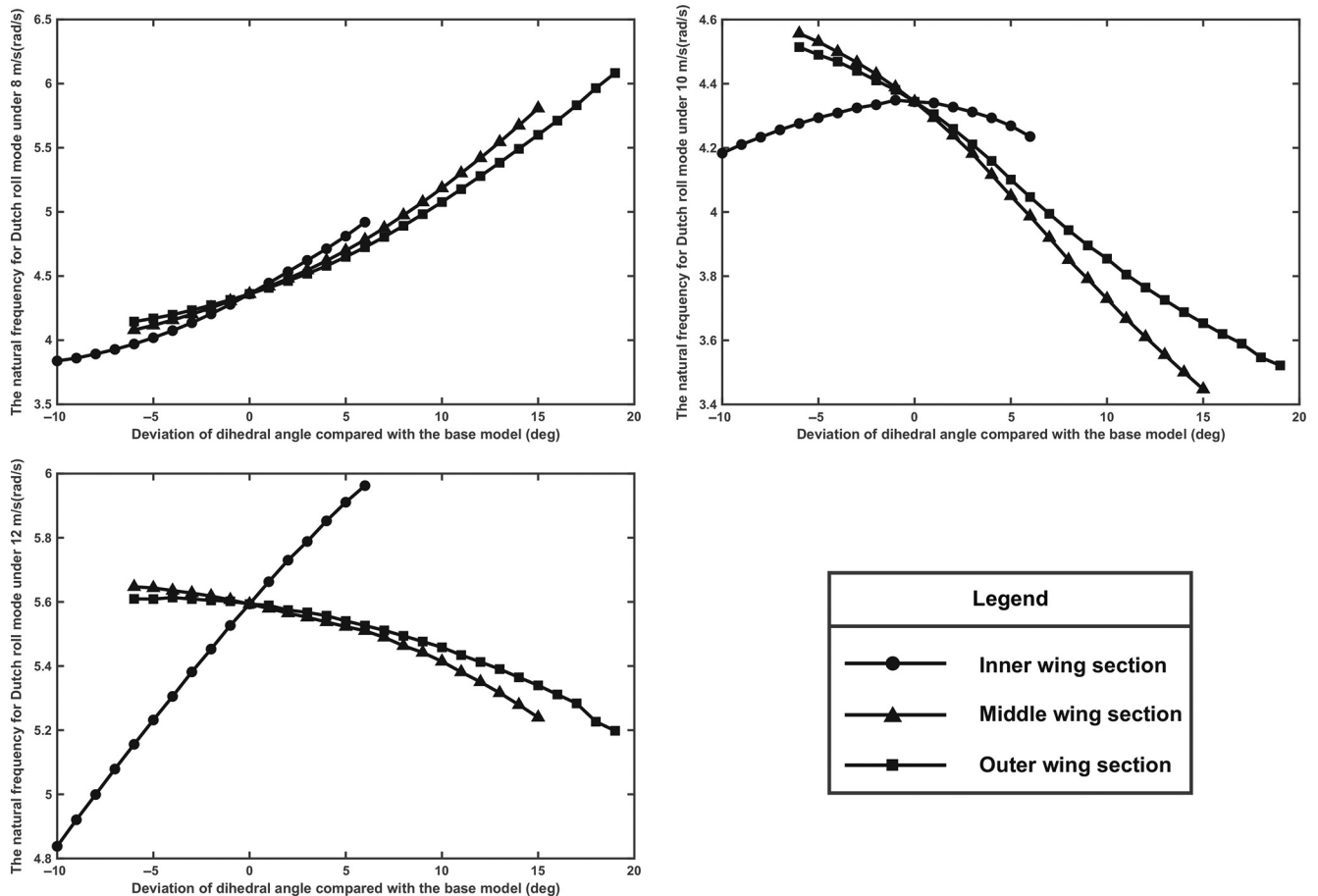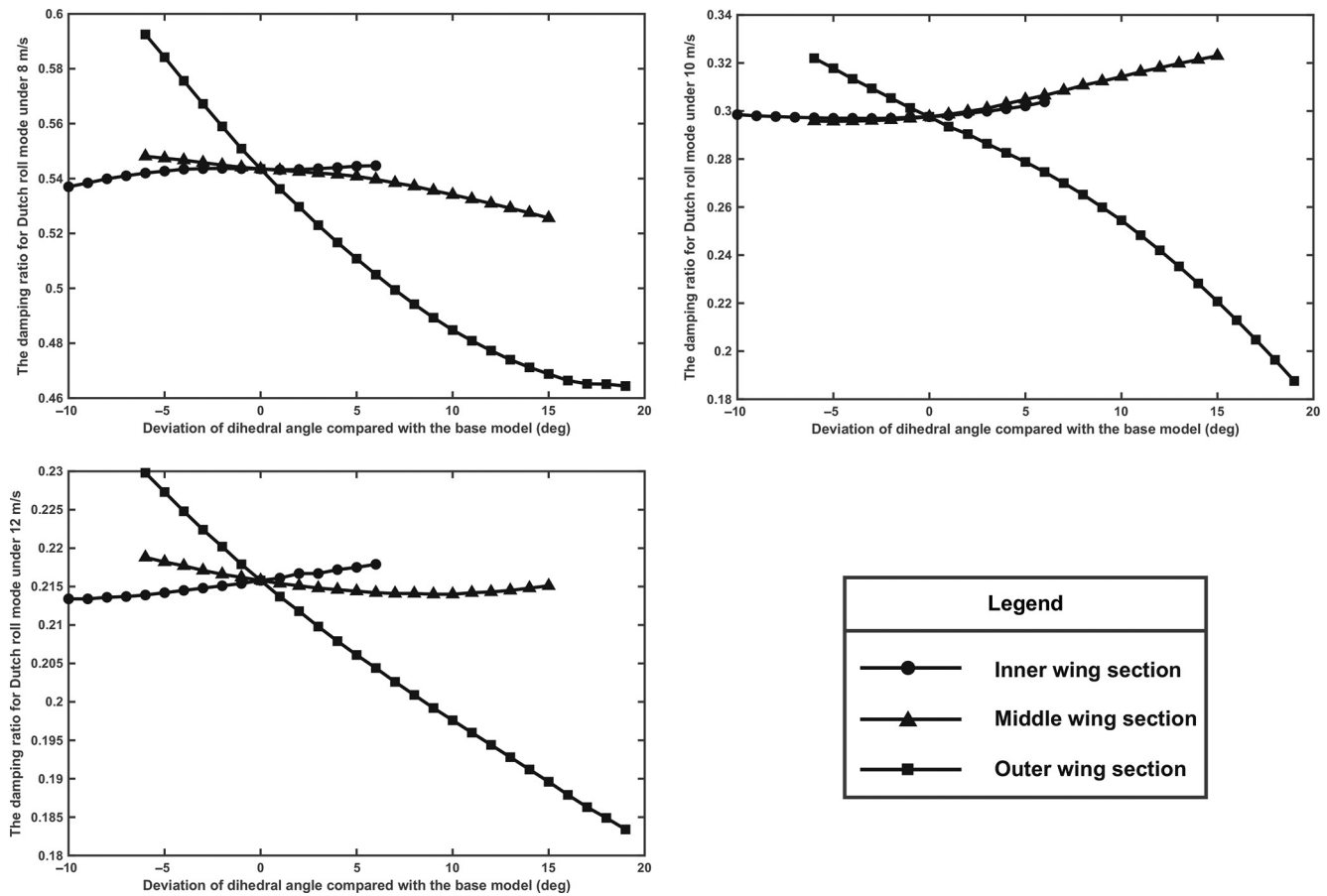
**Figure 8** Influence of dihedral angle changing on the damping ratio for Dutch roll mode



characteristics of the lateral-directional modes under different dihedral angle distributions were calculated and compared.

The results of the analysis of Dutch roll mode characteristic relevant to the variation of dihedral angle are shown in Figures 7, 8 and 9.

Figure 7 shows that with the increasement of the dihedral angle of middle and outer sections, the natural frequency decreases under 10 m/s and 12 m/s and increases under 8 m/s. In addition to the case of 10 m/s, the natural frequency increases with the increasing dihedral angle of inner section.

As shown in Figure 8, the dihedral angle changing of outer section has the most significant effect on the damping ratio. The damping ratio decreases with an increasement of the dihedral angle of outer section.
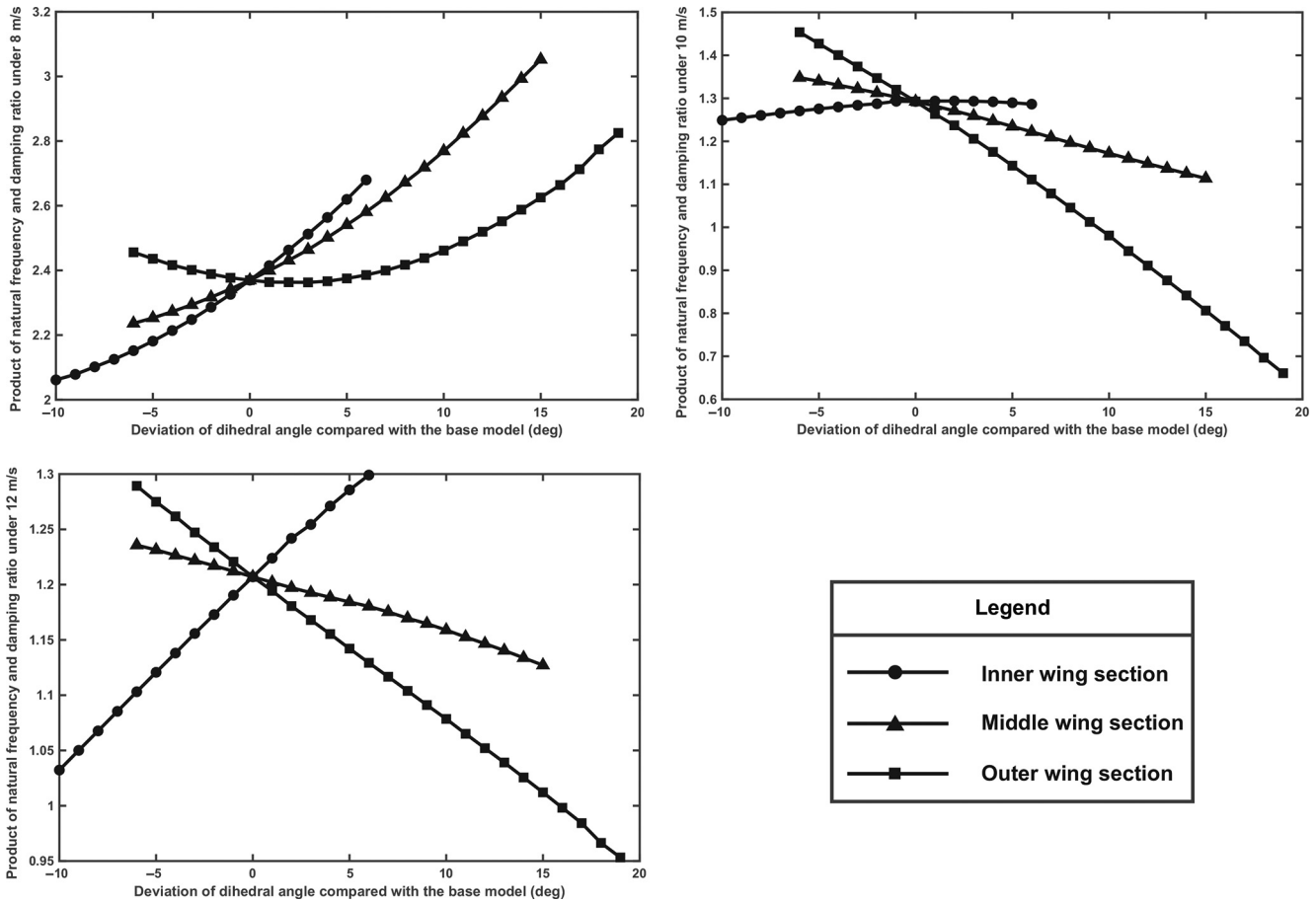
The results in Figure 9 show that for the whole gliding speed range, the product of the natural frequency and damping ratio increases with increasing inner wing section dihedral angle, which means that the motion convergence speed is rising. For airspeed values of 10 m/s and 12 m/s, the parameter decreases with the increasing dihedral angle in the middle and outer wing sections. For an airspeed of 8 m/s, a positive correlation was found between the parameter and the middle wing section dihedral angle. The product of the natural frequency and the damping ratio first decreases and then increases with an increasement in the outer wing section dihedral angle.

The eigenvalues are used as the assessment criteria for the spiral mode, and time constant is used as the assessment criteria for the rolling mode. The parameters relevant to the variation in the dihedral angle are shown in Figures 10 and 11. The results show that time constant decreases with the increasing dihedral angle of the outer section, which means that the motion convergence speed increases. Time constant changes slightly with the variation in the middle section dihedral angle. As the dihedral angle of the inner section increases, time constant rises. In summary, changes in the dihedral angle have only a slight effect on the rolling mode, and all of the analysed configurations have a well-convergent rolling mode.

For airspeeds of 10 m/s and 12 m/s, the eigenvalue of the spiral mode decreases with the increasing in the dihedral angle of each wing section, which means that the spiral mode tends to be convergent. For an airspeed of 8 m/s, the eigenvalue of the spiral mode first decreases and then increases with the increasement in the inner and middle section dihedral angles. According to Figure 11, the variation in the dihedral angle of the outer section has the most significant impact on the eigenvalue of the spiral mode.

A total of 9,724 configurations were analysed at various airspeeds. For the rolling mode, all the analysed configurations have a convergent rolling mode. It is worth noting that the products of the natural frequency and damping ratio for all of the configurations remain positive. This result indicates that

**Figure 9** Influence of dihedral angle changing on the product of natural frequency and damping ratio



convergent trend after a doublet aileron excitation. This convergent trend qualitatively proves the stability of the Dutch rolling mode. The natural frequency and the damping ratio are used to describe the Dutch roll mode. According to the sideslip angle data, the natural frequency and the damping ratio were identified using the fast fourier transform (FFT)-based half-power bandwidth method (Fu *et al.*, 2019). This method has been compared with the time-domain peak attenuation method in Fu's research (Fu *et al.*, 2019). The comparison results indicated the advantages of the FFT-based half-power bandwidth method when the aircraft oscillation mode identification is needed. Sampling frequency of the sideslip angle data is 25 Hz, and sampling time is 3.36 s. The identified results and the theoretical analysed results under 10 m/s combining the aircraft's moments of inertia are listed in Table 3.

It is worth noting that difference exists between the identified results and theoretical analysed results. Authors infers that in addition to aircraft manufacturing error, the main reason for the difference is that the influence of bird's body was neglected in the aerodynamic analysis. The body of the flight vehicle has a negative contribution to the aerodynamic derivatives including $C_{y\beta}$, $C_{n\beta}$. According to the flight mechanics theory, the approximations for Dutch roll mode's natural frequency and damping ratio (Robert C, 1998) are listed below:

Dutch roll mode is convergent for all of the configurations. A total of 7,436 configurations meet the requirements for level 1 Dutch roll mode criterion. This result suggests that the requirement for Dutch roll mode stability can be easily met for the configurations described in this study. This can support Sach's conclusion that bird is lateral-directional stable because of "size effect". For the spiral mode, 5,902 configurations have a convergent spiral mode with a negative eigenvalue. The results revealed that frigatebird can obtain a good lateral-directional mode characteristic by changing its wing dihedral angle.
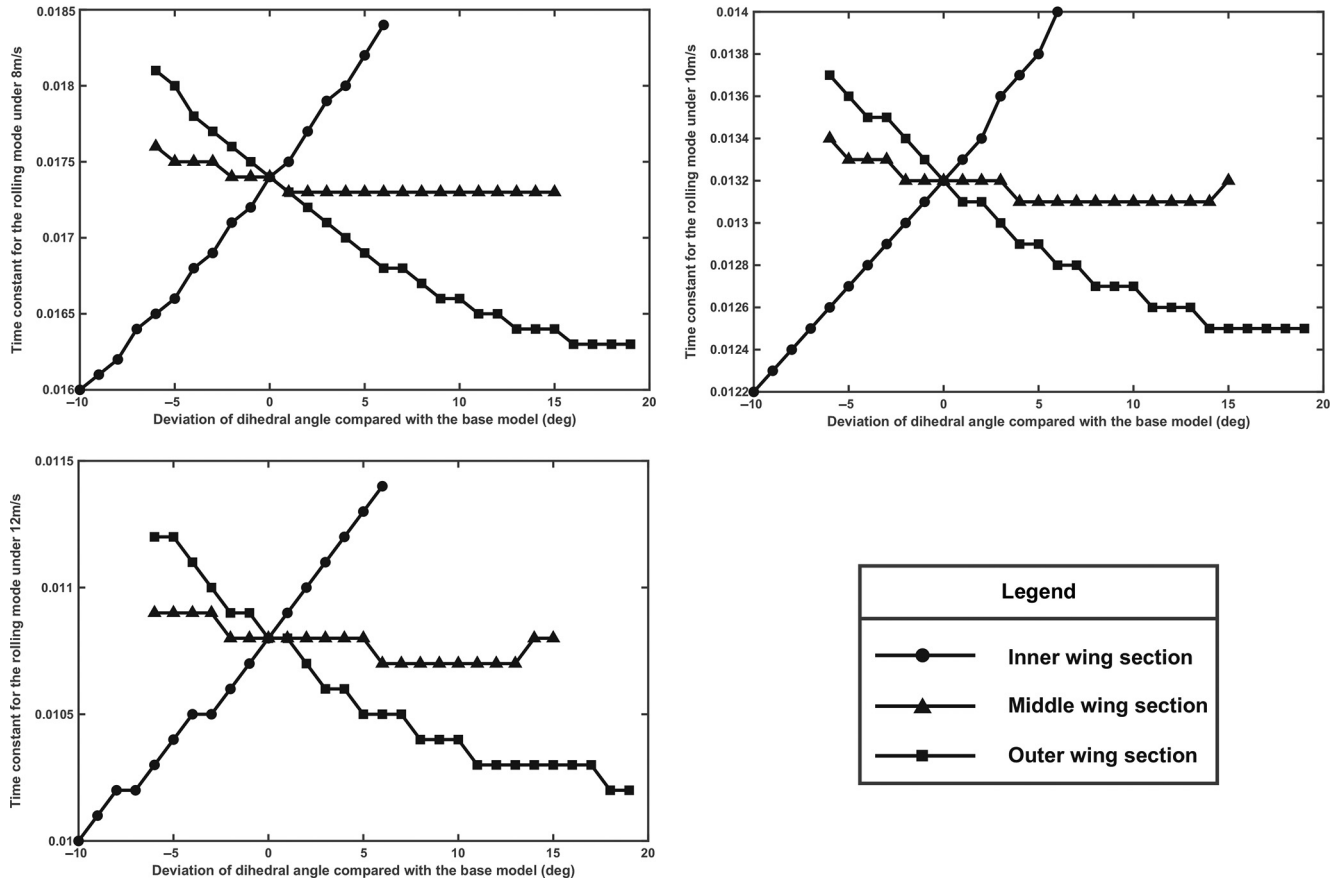
**Flight experiment result analysis**
Figure 12 shows the flight data of the glide with no lateral-directional control input. The data shows that the bird-inspired aircraft performs a gliding with the velocity of about 12 m/s. And the parameters for lateral-directional locomotion remain convergent. Considering that small disturbances (i.e. gust) exist in the atmosphere, the flight data indicated that the bird-inspired aircraft can perform a stable glide under the disturbances.

The flight data of the glide with a doublet aileron excitation was shown in the Figure 13. The data shows that a doublet aileron excitation was added on the bird-inspired aircraft when the speed is about 10 m/s. It can be seen that the lateral-directional flight parameters oscillate and then perform a

**Figure 10** Influence of dihedral angle changing on time constant for the rolling mode



$$\omega_n = \sqrt{\overline{N_\beta} - \overline{N_\beta}\overline{Y}_r + \overline{N}_r\overline{Y}_\beta} \qquad (3)$$

$$\xi = -\frac{\overline{N}_r + \overline{Y}_\beta}{2\omega_n} \qquad (4)$$

It can be found that with the decreasing of $C_{y\beta}$ and $C_{n\beta}$, the natural frequency tends to decrease and the damping ratio tends to increase. This deduction is consistent with the comparison results between the identified results and theoretical analysed results. Further study should incorporate the effects of the bird's body in the aerodynamic analysis. Although difference exists, the identified Dutch roll mode parameters indicated that the bird-inspired aircraft has a convergent Dutch roll mode. The identified results preliminarily prove the accuracy of the theoretical analysed results.

The FFT-based half-power bandwidth method developed by Fu was used to identified the natural frequency and the damping ratio in our work. After reviewing the method, we agreed that the sampling frequency, sampling time and amplitude-frequency diagram making would affect the uncertainties of the method.

As for the influence of sampling frequency, we decrease the sampling frequency from 25 Hz to 12.5 Hz and identified the

parameters. The results show that the damping ratio changes from 0.445 to 0.446, the natural frequency changes from 1.8713 to 1.848. The influence of sampling frequency is small.

As for the influence of sampling time, the conventional analysis method is to extend the sampling time by supplementing the data of stable convergent value. Considering that the sampling time in our experiment is short, the sideslip angle did not converge to a stable value at the end of sampling time. In this case, the artificial addition of data will have a great impact on the identified results. In Fu's research (Fu *et al.*, 2019), the influence of sampling time to results has been analysed. The results show that increasing sampling time help to make the results more accurate. Fu's analysis can serve as a reference to evaluate the influence of sampling time to the uncertainties of the method.

The uncertainties in making amplitude-frequency diagram mainly lies in determining the coordinates of half-power points. The more data points obtained in amplitude-frequency diagram, the more accurate the curve in the diagram is. Then, it would lead to a smaller uncertainty in the process of determining half-power points coordinates.

In summary, it is necessary to extend the sampling time and obtain more data points to reduce the uncertainties of the method.

**Figure 11** Influence of dihedral angle changing on the eigenvalue for the spiral mode
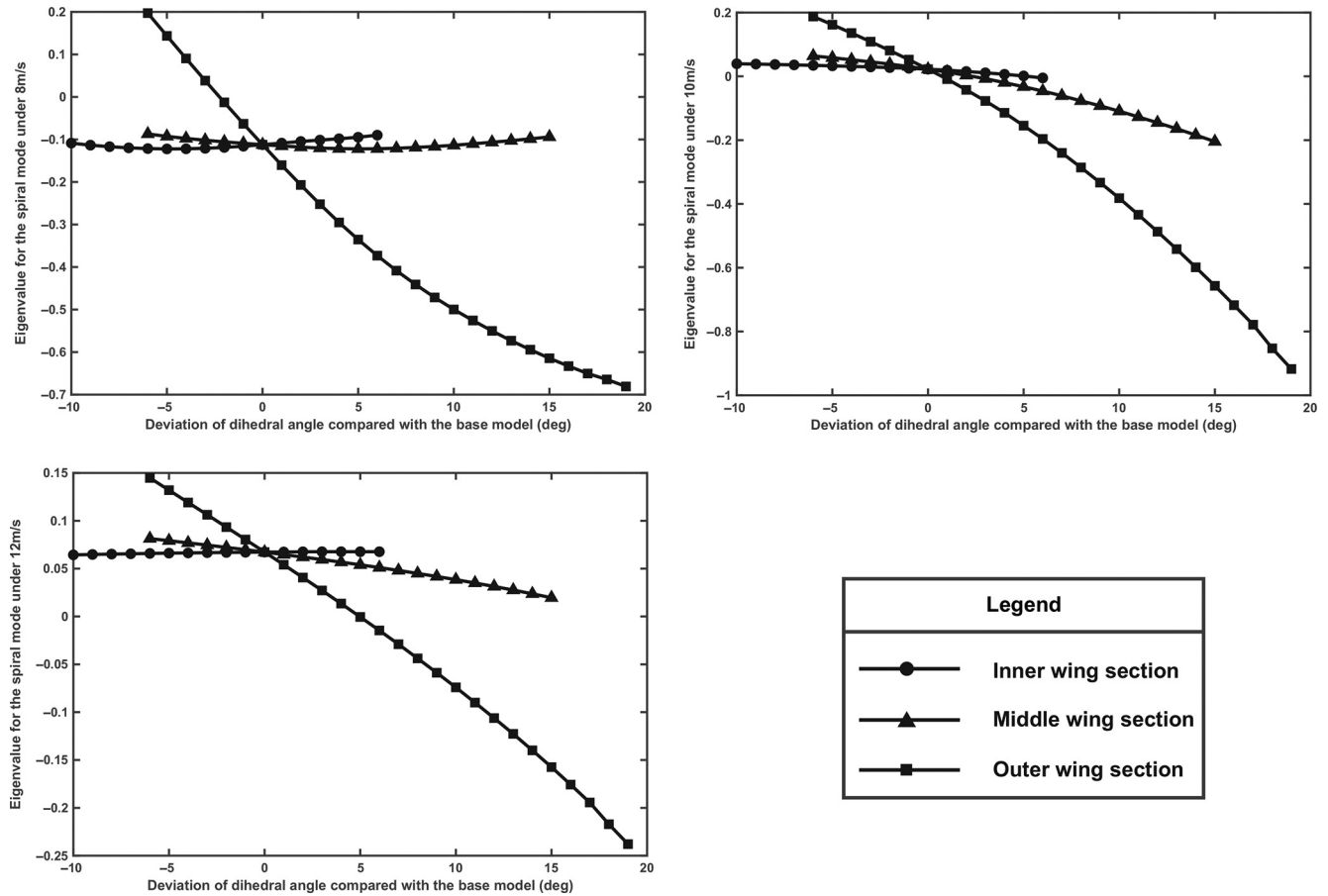


## Conclusion

In this paper, a geometric model and mass model of a gliding frigatebird were constructed. The characteristics of the lateral-directional modes for gliding frigatebird model were analysed. The influence of the dihedral angle on the lateral-directional dynamic stability of gliding frigatebirds was assessed by changing the dihedral angle of each wing section. A bird-inspired aircraft was developed, and the flight experiment was carried out to verify the lateral-directional stability of the model.

The analysis results show that Dutch roll mode of the gliding frigatebird base model remains convergent at airspeeds in the range of 8 m/s to 12 m/s. The values of the product of the natural frequency and damping ratio for Dutch roll mode of all the configurations are greater than 0.35 rad/s, which means that the convergent speed is high. When considering the natural frequency, the damping ratio and the product of these two parameters, about 76.5% of the analysed configurations meet the level 1 Dutch roll mode criterion. This result indicated that frigatebirds achieve Dutch roll mode dynamic stability more easily than aircraft without a vertical tail in general.

All of the configurations analysed in this paper have a convergent rolling mode and the convergence speed is high.

Changing the dihedral angle distribution has only a slight effect on the rolling mode at all of the analysed gliding speeds.

For the spiral mode, about 60.7% of the analysed configurations have a convergent spiral mode. In summary, frigatebird can achieve lateral-directional dynamic stability by changing its dihedral angle spanwise distribution. Considering that the Dutch roll mode and rolling mode are convergent in this paper, it is inferred that the key role of the dihedral angle spanwise distribution changing is to achieve a convergent spiral mode.

The flight data of the glide with no lateral-directional control input suggests that the bird-inspired aircraft can perform stable gliding. The natural frequency and damping ratio of the Dutch roll mode were identified based on the sideslip angle data of the glide with a doublet aileron excitation. Although difference exists between the identified results and theoretical analysed results, the Dutch roll mode is proved to be convergent by the identified results.

In our work, gliding frigatebird was treated as a rigid body and its lateral-directional dynamic stability was analysed. Considering that no essential difference exists in the gliding morphology of nature birds, nature birds could be regarded as fixed-wing aircraft having different wing configurations without a vertical stabilizer. Thus, it can be concluded that our model has wide applicability to analysis the stability of these gliding birds.

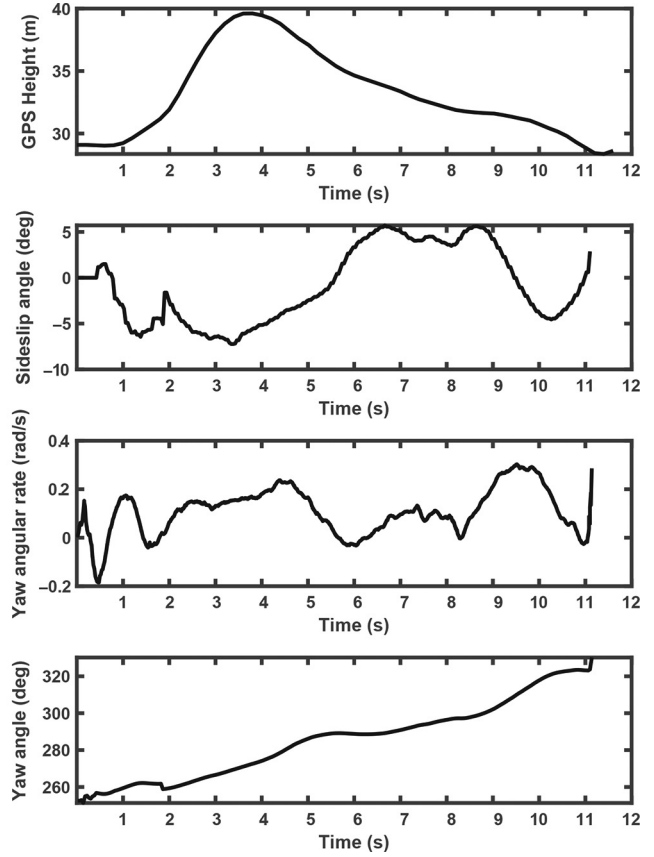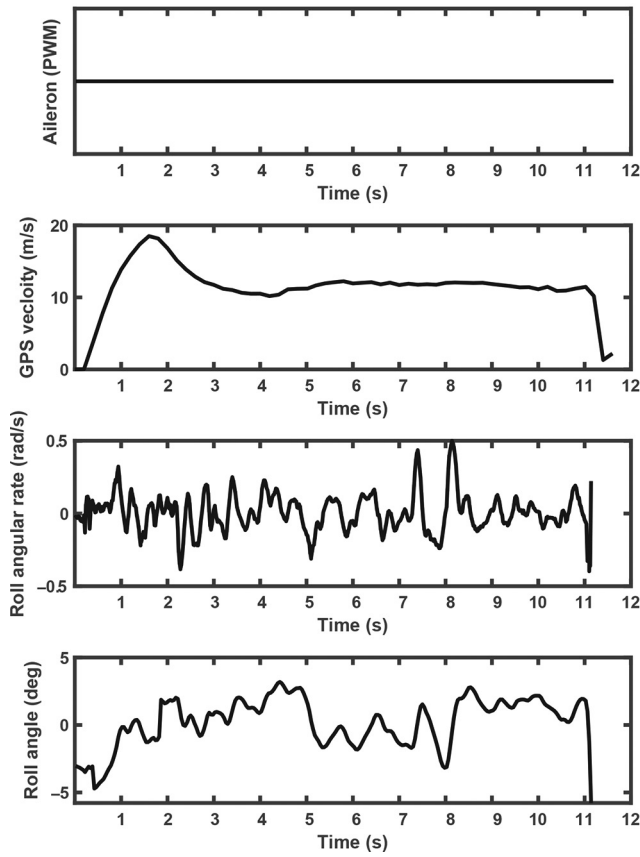**Figure 12** Flight data of the glide with no lateral-directional control input



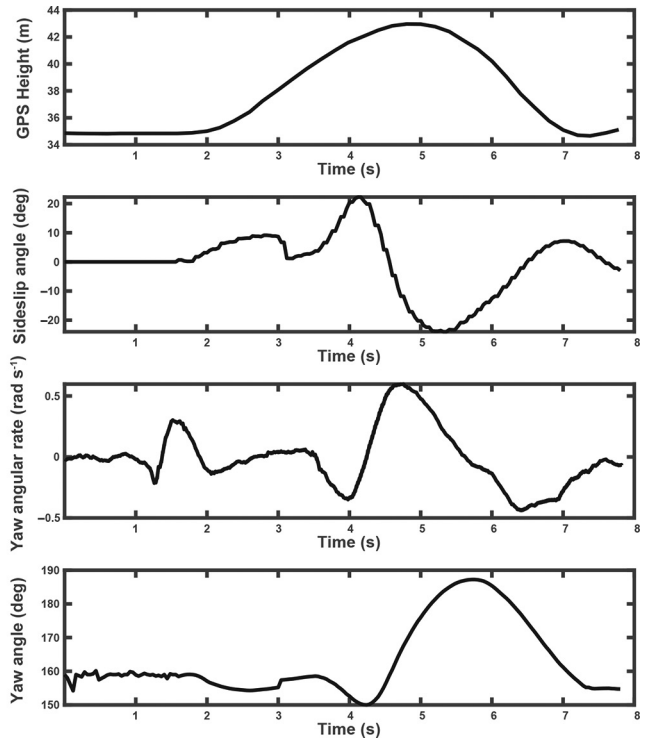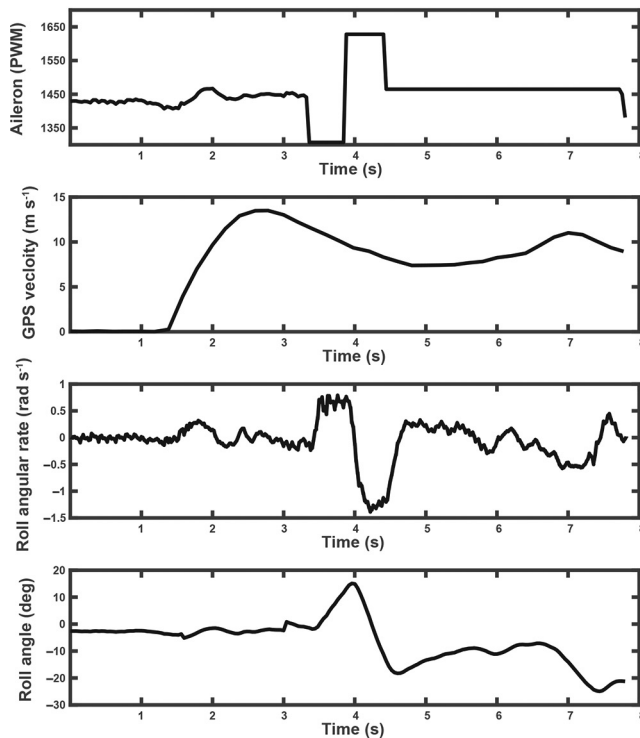**Figure 13** Flight data of the glide with a doublet aileron excitation

**Table 3** Results comparison for the Dutch roll mode characteristic

| Identified results | | | Theoretical analysed results | | |
|---|---|---|---|---|---|
| The natural frequency (rad/s) | The damping ratio | The product of natural frequency and damping ratio | The natural frequency (rad/s) | The damping ratio | The product of natural frequency and damping ratio |
| **1.8713** | 0.445 | 0.8327 | 2.6258 | 0.1793 | 0.4708 |

## References

Abdulrahim, M. and Lind, R. (2004), "Flight testing and response characteristics of a variable gull-wing morphing aircraft", *American Institute of Aeronautics and Astronautics*.

Anderson, J.D. (2017), *Fundamentals of Aerodynamics*, McGraw-Hill Education, New York, NY.

Brewer, M.L. and Hertel, F. (2007), "Wing morphology and flight behavior of pelecaniform seabirds", *Journal of Morphology*, Vol. 268 No. 10, pp. 866-877.

Brown, R.H.J. (1963), "The flight of birds", *Biological Reviews*, Vol. 38 No. 4, pp. 460-489.

Chatterjee, S. and Templin, R.J. (2007), "Biplane wing planform and flight performance of the feathered dinosaur microraptor gui", *Proceedings of the National Academy of Sciences*, Vol. 104 No. 5, pp. 1576-1580.

Cooper, G.E. and Harper, R.P.J. (1969), "The use of pilot rating in the evaluation of aircraft handling qualities", NASA-TN-D-5153.

Dhawan, S. (1991), "Bird flight", *Sadhana*, Vol. 16 No. 4, pp. 275-352.

Etkin, B. and Reid, L.D. (1996), *Dynamics of Flight: Stability and Control*, John Wiley & Sons, New York, NY.

Freguson-Lees, J. and Christie, D.A. (2006), *Raptors of the World*, Princeton University Press, Princeton.

Fu, J., Huang, J., Wang, L. and Song, L. (2019), "Oscillation mode flight data analysis based on FFT", *Aircraft Engineering and Aerospace Technology*, Vol. 91 No. 1, pp. 157-162.

Gillies, J.A., Thomas, A.L.R. and Taylor, G.K. (2011), "Soaring and manoeuvring flight of a steppe eagle aquila nipalensis", *Journal of Avian Biology*, Vol. 42 No. 5, pp. 377-386.

Hamershock, D.M., Seamans, T.W. and Bernhardt, G.E. (1992), "Determination of body density for twelve bird species", Flight Dynamics Directorate Wright Laboratory, WL-TR-93-3049.

Herzog, K. (1968), *Anatomie Und Flugbiologie Der Vögel*, Gustav Fischer Verlag, Stuttgart.

Hoak, D.E. (1978), "The USAF stability and control DATCOM", Air force flight dynamics laboratory.

Hoey, R.G. (1992), "Research on the stability and control of soaring birds", *28th National Heat Transfer Conference*, American Institute of Aeronautics and Astronautics.

Koehl, M.A.R., Evangelista, D. and Yang, K. (2011), "Using physical models to study the gliding performance of extinct animals", *Integrative and Comparative Biology*, Vol. 51 No. 6, pp. 1002-1018.

Kuroda, N. (2004), "Fragmental notes on avian morpho-anatomy", *Journal of the Yamashina Institute for Ornithology*, Vol. 35 No. 2, pp. 207-219.

Lentink, D., Müller, U.K., Stamhuis, E.J., de Kat, R., van Gestel, W., Veldhuis, L.L.M., Henningsson, P., Hedenström, A., Videler, J.J. and van Leeuwen, J.L. (2007), "How swifts control their glide performance with morphing wings", *Nature*, Vol. 446 No. 7139, p. 1082.

Marchant, S. and Higgins, P. (1990), *Handbook of Australian and New Zealand Birds*, Oxford University Press, Oxford.

Melin, T. (2000), "A vortex lattice MATLAB implementation for linear aerodynamic wing applications", Master Thesis, Kungliga Tekniska Högskolan (KTH).

Muir, R.E., Arredondo-Galeana, A. and Viola, I.M. (2017), "The leading-edge vortex of swift wing-shaped delta wings", *Royal Society Open Science*, Vol. 4 No. 8.

Pennycuick, C. (1983), "Thermal soaring compared in three dissimilar tropical bird species, fregata magnificens, pelecanus occidentalis and coragyps atratus", *Journal of Experimental Biology*, Vol. 102 No. 1, pp. 307-325.

Pennycuick, C.J. (2008), *Modelling the Flying Bird*, Academic Press, Cambridge.

Prosser, C.F. and Wiler, C.D. (1976), "RPV flying qualities design criteria", Air Force Flight Dynamics Laboratory, AFFDL-TR-76-125.

Robert, C.N. (1998), *Flight Stability and Automatic Control*, McGraw-Hill Education, New York, NY.

Rogalla, S., Nicolaï, M.P.J., Porchetta, S., Glabeke, G., Battistella, C., D'Alba, L., Gianneschi, N.C., van Beeck, J. and Shawkey, M.D. (2021), "The evolution of darker wings in seabirds in relation to temperature-dependent flight efficiency", *Journal of the Royal Society Interface*, Vol. 18 No. 180, p. 20210236.

Sachs, G. (2005), "Yaw stability in gliding birds", *Journal of Ornithology*, Vol. 146 No. 3, pp. 191-199.

Sachs, G. and Moelyadi, M.A. (2010), "CFD based determination of aerodynamic effects on birds with extremely large dihedral", *Journal of Bionic Engineering*, Vol. 7 No. 1, pp. 95-101.

Schmitz, A., Ondreka, N., Poleschinski, J., Fischer, D., Schmitz, H., Klein, A., Bleckmann, H. and Bruecker, C. (2018), "The peregrine falcon's rapid dive: on the adaptedness of the arm skeleton and shoulder girdle", *Journal of Comparative Physiology A*, Vol. 204 No. 8, pp. 747-759.

Smith, A.J.W. (1984), *Biophysical Aerodynamics and the Natural Environment*, John Wiley & Sons, New York, NY.

Smith, J.M. (1952), "The importance of the nervous system in the evolution of animal flight", *Evolution*, Vol. 6 No. 1, pp. 127-129.

Song, L., Yang, H. and Zhang, Y. (2014), "Dihedral influence on lateral-directional dynamic stability on large aspect ratio tailless flying wing aircraft", *Chinese Journal of Aeronautics*, Vol. 27 No. 5, pp. 1149-1155.

Song, L., Yang, H., Yan, X. and Huang, J. (2015), "Increasing the flying wing lateral-directional dynamic stability without relying on augmentation system", *Systems Engineering and Electronics*, Vol. 37 No. 11, pp. 2561-2565.

Song, L., Yang, H. and Xie, J. (2016), "Method for improving the natural lateral-directional stability of flying wings", *Journal of Aerospace Engineering*, Vol. 29 No. 5, p. 616003.

Videler, J.J., Stamhuis, E.J. and Povel, G. (2004), "Leading-edge vortex lifts swifts", *Science*, Vol. 306 No. 5703, pp. 1960-1962.

Weimerskirch, H., Bishop, C., Jeanniard Du Dot, T., Prudor, A. and Sachs, G. (2016), "Frigate birds track atmospheric conditions over months-long transoceanic flights", *Science*, Vol. 353 No. 6294, pp. 74-78.

Whittow, G.C. (1999), *Sturkie's Avian Physiology*, Academic Press, San Diego.

Zheng, G. (2012), *Ornithology*, Beijing Normal University Press, Beijing.

## Corresponding author

**Lei Song** can be contacted at: songlei@buaa.edu.cn